

RESEARCH ARTICLE

Tracking *in vitro* and *in vivo* siRNA electrotransfer in tumor cells

Aurelie Paganin-Gioanni¹, Elisabeth Bellard¹, Bettina Couderc², Justin Teissié^{1,*} and Muriel Golzio^{1,*}

¹IPBS CNRS (UMR 5089 Université de Toulouse III, CNRS), 205 Route de Narbonne, 31077 Toulouse France, ²Université de Toulouse III ; Institut C. Regaud, 20-24 rue du Pont ST Pierre, 31052 Toulouse France.

*Correspondence to: Muriel Golzio and Justin Teissié, Email: muriel.golzio@ipbs.fr (MG) or justin.teissie@ipbs.fr (JT), Tel: +33 561 175812/13; Fax: +33 561 175994

Received 29 April 2008; Revised 15 May 2008; Accepted 20 May 2008; Published online 27 May 2008

J RNAi Gene Silenc (2008), 4(1), 281-288

© Copyright The Authors: This is an open access article, published under the terms of the Creative Commons Attribution Non-Commercial License (<http://creativecommons.org/licenses/by-nc/2.0/uk/>). This license permits non-commercial use, distribution and reproduction of the article, provided the original work is appropriately acknowledged with correct citation details.

ABSTRACT

RNA interference-mediated gene silencing offers the potential of targeted inhibition of disease-relevant genes. *In vivo* delivery of RNAi reagents can be obtained by a variety of approaches. Physical delivery methods appear safer and lack side effects. Electro-permeabilization is one of the non-viral methods successfully used to transfer small interfering RNAs (siRNAs) *in vitro* and *in vivo*. A promising approach may be, very little is known about the fundamental processes mediating siRNA transfer. In this study, we have investigated cellular delivery pathways involved in electro-delivery of siRNAs by a direct fluorescence imaging method. An Alexa-labeled siRNA was electro-transferred into murine melanoma cells stably-expressing the enhanced green fluorescent protein (eGFP) target reporter gene. The silencing of eGFP gene expression was quantified by time-lapsed fluorescence microscopy. Fluorescently-labeled siRNAs were found distributed homogeneously in cytoplasm 48 hours after electro-transfer, apparently by diffusion. Furthermore, siRNAs showed homogeneous distribution *in vivo* 48 hrs after intra-tumoral injection followed by electro-permeabilization. Histological fluorescence microscopy showed that siRNAs were mostly localized in the cytoplasm. Overall, this study shows that electro-permeabilization facilitates cytoplasmic distribution of siRNA, both in cultured cells and *in vivo*. This method offers a potential therapeutic tool to facilitate direct siRNA penetration into solid tumors.

KEYWORDS: Electro-permeabilization, electro-poration, RNAi, tumors, fluorescence microscopy

INTRODUCTION

RNA interference offers a powerful approach to silence post-transcriptional gene expression (Fire et al, 1998) and thus have considerable therapeutic potential (Novina and Sharp, 2004; Akhtar and Benter, 2007). The future use of siRNA as therapeutics will largely rely on the development of efficient *in vivo* delivery methods, which remains a major challenge (Rossi, 2005; Ryther et al, 2005; Aigner, 2007). A safe siRNA delivery approach requires direct transfer of molecules to the cytoplasm,

avoiding off-target interactions associated with the cellular uptake pathways (Heidel et al, 2004). Electric pulses are known to strongly stimulate cellular uptake of various drugs that otherwise show intrinsically poor cellular delivery. Electric pulses have also been frequently used to deliver drug, siRNAs and plasmids into organs and tissues, *in vivo* (Li, 2004; Wells, 2004; Golzio et al, 2005; Golzio et al, 2007). In rodents, electric pulses have been used to deliver siRNAs into various organs, such as skin (Zhang et al, 2002), eyes (Matsuda and Cepko, 2004), brain (Akaneya et al, 2005), muscles (Golzio et al, 2005;

Kishida et al, 2004), joint tissue (Inoue et al, 2005) and kidneys (Takabatake et al, 2005). However, electro-delivery of large nucleic acids (e.g., plasmids) is less efficient in solid tumors (Rols et al, 1998; Coralli et al, 2001; Cemazar et al, 2002). Electro-delivery offers several specific advantages: for example, delivery of molecules is restricted to the volume where the electric field is generated (Miklavcic et al, 1998); pulse parameters are fully and easily controlled; very few side effects have been reported for these treatments emphasizing the suitability of this physical method for clinical use.

Studies on electro-chemotherapy and electro-gentherapy to enhance the delivery of small molecule drugs and nucleic acids, respectively, are currently underway (e.g., ESOPe and Angioskin European projects). Previously, we generated B16-F10 melanoma cell line stably-expressing enhanced green fluorescent protein (eGFP) and showed that electrical treatment led to siRNA-mediated endogenous gene silencing in solid tumors (Golzio et al, 2007). In this study, in order to assess the intra-cellular distribution of siRNAs, we compared *in vitro* and *in vivo* efficacy in gene silencing by electro-transferred fluorescent and non fluorescent siRNA. We then followed the intra-cellular localization of fluorescently-labeled siRNA in cultured cells and in solid tumors, *in vivo*.

MATERIALS AND METHODS

Cell culture

B16-F10 melanoma cells expressing the enhanced Green fluorescent protein (B16F10-eGFP), produced by retroviral transduction (see Cemazar et al, 2006) were maintained in Eagle's minimum essential medium (EMEM; Gibco-Invitrogen, USA) with 10% (v/v) foetal calf serum (Gibco), penicillin (100 units/ml, Gibco-Invitrogen), streptomycin (100 mg/ml, Gibco-Invitrogen) and L-glutamine (0.58 mg/ml, Eurobio, France) in a 5% (v/v) CO₂ humidified incubator at 37°C (Jouan, France).

siRNAs

All siRNAs were purchased from Qiagen Xeragon (USA). The eGFP22 siRNA (sense: 5'GCAAGCUGACCCUGAA GUUCAU, antisense: 5'GAACUUCAGGGUCAGCUUG CCG) was directed against eGFP mRNA and was designed according to Caplen and coworkers (Caplen et al, 2001). To determine the localization of siRNA, a fluorescent Alexa Fluor 546 labeled siRNA was used. The P76 siRNA (sense: 5'GCGGAGUGGCCUGCAGGUA dTdT, antisense: 5' UACCUGCAGGCCACUCCGC dTdT) was directed against an unrelated human mRNA and shows no significant homology to mouse transcripts according to Basic Local Alignment Search Tool analysis. It was used as a control for specificity of the siRNA constructs.

Permeabilization of cultured cells and electro-transfer of siRNAs

The penetration of Propidium Iodide (100 µM in a pulsing buffer: 10 mM phosphate, 1 mM MgCl₂, 250 mM sucrose, pH 7.4) (Sigma) was used to monitor permeabilization. 100 µl of the cell suspension (i.e., 5x10⁵ cells) in the pulsing buffer was placed in electro-pulsation chamber, which was

designed using stainless steel parallel plates electrodes (10 mm length, 0.5 mm thick and 4 mm inter-electrode distance) brought in contact to the bottom of a 35 mm Petri dish (Nunc, Denmark). Electro-pulsation (EP) was operated by using a CNRS cell electro-pulsator (Jouan), which delivered square-wave electric pulses. An oscilloscope (Enertec, France) monitored pulse shape online. A uniform electric field was generated when the voltage pulse was delivered. Ten pulses with controlled duration of 5 ms, at a frequency of 1 Hz, were applied at preset electric field intensities at room temperature (25°C). Membrane re-sealing occurred 5 min after pulse application, keeping internalized dyes trapped. Cells were analyzed by flow cytometry (Becton Dickinson FACScan) to determine the percentage of permeabilized cells (i.e., fluorescent cells). Cell viability 24 hrs after the treatment was determined by coloration using Crystal Violet (Merck, Germany).

Electro-transfer of siRNAs was performed using optimum parameters for cell permeabilization. Cells in suspension (5x10⁵ cells) were transfected with 2 µg of siRNA in pulsing buffer under the same conditions as for permeabilization. Cells were then analyzed by flow cytometry in order to determine the percentage of cells expressing the eGFP, and their associated fluorescence intensity. Cells were then treated with siRNAs and electrical pulses, and were sorted out by flow cytometry (FACScalibur, Becton Dickinson) 48 hrs after treatment to identify silenced cells with silenced eGFP. Selected cells were observed under a microscope.

Cell Viability analysis

Cell viability was determined by the ability of cells to grow and divide over a 24 hour period (Gabriel and Teissie, 1995). Cells were pulsed, kept for 10 min at 30°C and then grown on Petri dishes after adding 1 ml of culture medium for 24 hrs at 37°C, in a 5% (v/v) CO₂ incubator. Viability was measured by counting cells with the coloration method as above.

Mouse tumor model

Female C57Bl/6 mice were obtained from Rene Janvier (St Isle, France) and were subjected to an adaptation period of at least 10 days before experimentation. They were maintained at a constant room temperature with a 12 hrs light cycle in a conventional animal facility. The mice were 10-14 weeks old at the beginning of the experiments weighing 20-25 g. Tumors were implanted subcutaneously in the right flank of the mice by inoculation of 10⁶ B16F10-eGFP cells in PBS and grown to a size of 5-7 mm in diameter. All procedures were performed with approved protocols, in accordance with the French CNRS and EU commission regulations for laboratory animals' care.

In vivo electro-pulsation

Fifty µl of saline solution (i.e., PBS containing 40 U of the RNase inhibitor, RNasin) (Promega, USA) and either 12 µg of eGFP22 or of p76 siRNA were slowly injected (for about 15 sec) with a Hamilton syringe through a 26G needle (Hamilton, Switzerland) into the tumor, under 2% (v/v) isoflurane anesthesia. In the control conditions, the volume of siRNA was replaced by siRNA suspension buffer to keep the injection conditions similar. Electro-

pulsation was applied 30 sec after injection. Parallel plate electrodes (length 1 cm, width 0.6 mm, inter-electrode distance 6 mm) (IGEA, Italy) were fitted around the tumor that had been previously shaved with a cream (Veet, Reckitt & Colman, France). A good electric contact was achieved between the skin and the electrodes using a conducting paste (Eko-gel, Italy). Electrical parameters were defined by taking pulse duration into special consideration, which appears critical for nucleic acid electro-transfer. Pulses with reverse polarities were also used to help electro-delivery by taking advantage of the vectorial character of the electric field. Square-waved pulses were delivered as described previously (Golzio et al, 2007; 480 V, 5 ms, 1 Hz). A sequence of four pulses was applied, followed by additional four pulses with the reverse polarity. An electronic switch cut the pulse as soon as their intensity reached 5A to protect against current surges.

Non-invasive stereomicroscopic fluorescence imaging of live animals

GFP expression in the tumor cells was detected directly through the skin in the anesthetized animal by digitized fluorescence stereomicroscopy. This procedure allowed observation of GFP expression in the same animal for several days. Briefly, mice were anesthetized with 2% (v/v) of isoflurane and were kept under anesthesia during the whole procedure. High-magnification images were obtained with an epifluorescence stereomicroscope using 0.8 magnification (Leica MZFL III, Germany) and a cooled CCD camera (Coolsnap fx, Roper Scientific, France) as previously described (Golzio et al, 2005). A 15 mm² part of the animal was observed, which covered the whole tumor. Camera was driven by the MetaVue software 2.6 (Molecular Devices Corporation, USA) from a PC (Dell, France). The exposure time was set at 1 sec with no binning. The fluorescence emission was obtained with a HBO lamp (Osram, Germany), using either a GFP or a G filter set (Leica Microsystems, Germany). The eGFP fluorescence from the tumor was measured quantitatively for one week, while the Alexa Fluor 546 labeled siRNA was detected *ex vivo* 48 hr after the treatment.

Histological sectioning

Mice were sacrificed by cervical dislocation at 48 hrs and tumors were rapidly observed by stereomicroscopy. The tissue was then mounted in the optimum cutting temperature (OCT) compound (Tissue-Tek, Sakura Finetek, NL), and was frozen in liquid nitrogen and pentane. Thin sections were cut at a 15 μ m thickness from the OCT compound blocks using a cryostat (Leica CM3050 S) at -20°C.

Confocal fluorescence microscopy

Cells and histological sections of tumors were visualized by confocal microscopy. GFP and Alexa Fluor 546 signals were detected with Zeiss LMS inverted confocal microscope equipped with a 488 nm laser for the GFP and with a 514 nm laser for the Alexa Fluor 546, using a Zeiss X40 objective (1.3 numerical aperture, oil immersion). Laser power and photomultiplier setting were kept identical for all samples to make the results comparable. Images were recorded and analyzed with the Zeiss LMS510 software (EMBL, Germany).

Statistical analysis

For each condition, 3 to 5 independent experiments were performed. Differences in percentages or relative fluorescence levels between the various conditions were statistically compared by using unpaired Student t-test two-sided using Microsoft Excel software. *0,05<P≤0,1, ** 0.01<P≤0.05 and ***P≤0.01.

RESULTS

In vitro cell permeabilization and cell viability

Permeabilization of cells was performed by application of long duration electric pulses (EP), which are required to load macromolecules into cells. Permeabilization of B16F10 cells was only detected for electric field values higher than a threshold. The threshold value was between 300 and 400 V/cm (Figure 1). At the optimum electric field intensity (600 V/cm), cell viability (V=95%) was preserved while a large fraction of cells was permeabilized (P= 57%). The percentage of viable permeabilized cells PV was 52% +/-15 (PV=P+V-100, i.e. (95%-100)+57%) (Teissie et al, 1999).

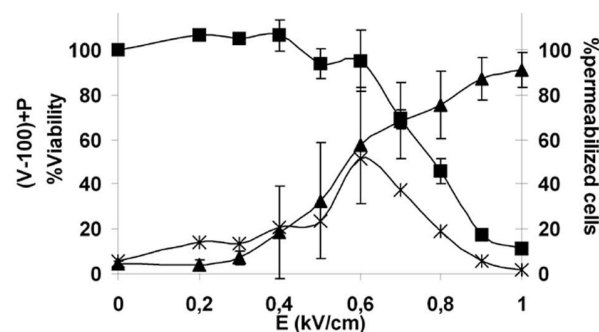


Figure 1. Electric field intensity effect on permeabilization and viability. Percentages of permeabilized cells, cell viability and viable permeabilized cells were plotted as a function of the electric field intensity. Permeabilization was assayed by the penetration of PI in cells and analyzed by flow cytometry (▲). The live cells were determined 24 hrs after the treatment by crystal violet coloration (■). Error bars represent standard deviation. The percentage of viable permeabilized cells were determined by calculating (permeabilization (%)+viability(%)-100).

In vitro electrotransfer of siRNAs

The transfer of the eGFP22 siRNA was carried out by electroporation of cells in suspension. We chose the electric field value of 600 V/cm shown to give a high number of permeabilized and viable cells. The percentage of cells expressing eGFP (GFP positive cells) was quantified as function of time (data not shown). Figure 2 shows relative percentage of cells expressing eGFP 48 hrs after a single treatment as well as the change in mean fluorescence intensity.

In all control experiments, relative percentages of cells expressing the eGFP were not significantly changed (Figure 2). Indeed, if an unrelated non-silencing siRNA

(negative siRNA) was electrotransferred, no changes in the percentage of eGFP positive cells were detected. As expected, the electrical treatment itself (+EP) had no effect. If eGFP22 siRNA (*i.e.* anti-eGFP siRNA Alexa Fluor 546 or anti-eGFP siRNA) was injected without EP application, no reduction in the percentage of GFP positive cells was observed. When the eGFP22 siRNA were electrotransferred (siRNA injection+ EP), a significant decrease in the percentage of eGFP positive cells were observed. The decrease was maximal from days 2 to 4 (data not shown). At day 2, the percentage of cells expressing eGFP decreased to 57.8%±3 for treatment with unlabeled siRNA and to 50.8%±3 for the Alexa labeled siRNA. The relative mean fluorescence intensity of the population decreased to 45.2%±3 for the unlabeled siRNA and to 45.8%±3 for the Alexa labeled siRNA, while the relative mean fluorescence intensity of eGFP positive cells did not show any detectable change. The effect of siRNA was found to be transient. The percentage of cells expressing eGFP returned to its initial value at day 7 post-treatment (data not shown). Alexa labeled siRNA electrotransfer (siRNA anti-eGFP Alexa Fluor 546+EP) showed the same silencing efficacy on the eGFP expression as unlabeled siRNA (Figure 2). This observation validated its reliable use in further experiments for the visualization of its localization within cells.

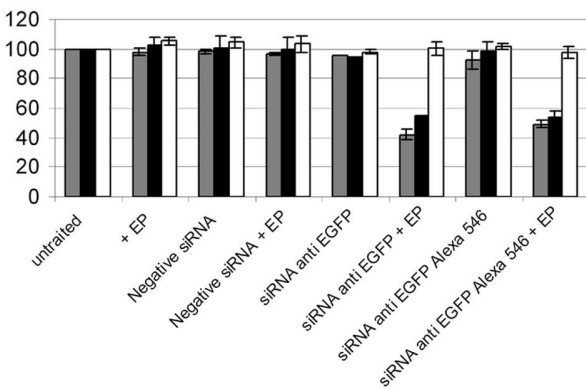


Figure 2. Level of silencing by siRNAs *in vitro* at 48 hrs. Cells in suspension were incubated in the presence of 1.4 μ M siRNA (either negative siRNA or anti-GFP siRNA, labeled with Alexa Fluor 546 or unlabelled) in pulsing buffer. Ten pulses of 5 ms at frequency of 1 Hz were applied at 0.7 kV/cm (+EP). Grey bars represent relative percentage of GFP expressing cells quantified at 48 hrs by flow cytometry. Black bars represent mean fluorescence intensity (IF) of the cell population relative to that of untreated cells. White bars show mean fluorescence intensity of cells, which remain GFP positive after electropulsation relative to the one of untreated cells. Error bars represent standard deviation.

Localization of the siRNA into cells after electrotransfer *in vitro*

Forty eight hours after pulsing cells with siRNA, eGFP negative cells were sorted out by flow cytometry. These cells were observed by confocal microscopy to visualize the labeled siRNA localization within cells and to evaluate eGFP expression. The results were compared with cells

simply incubated with the siRNA (Figure 3). No Alexa signal was detected in non-pulsed cells (-EP) (Figure 3, upper panels). After electrotransfer of siRNA labeled with Alexa Fluor 546 in cells (+EP), eGFP signal in cells reduced as compared with the control cells. Alexa signal was observed only in the cytoplasm (Figure 3, lower panels). A strong nuclear labeling of a few 'dead' tumor cells was observed, suggesting interaction between the siRNA or the Alexa Fluor 546 and the DNA of dead cells. Thus a decrease in the fluorescence intensity of eGFP indicates that electropermeabilization resulted in free cellular loading of labeled siRNA in active form.

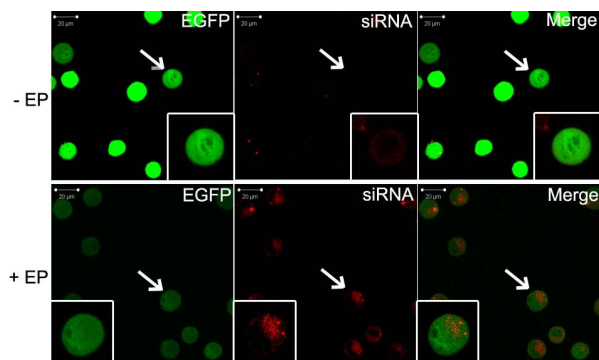


Figure 3. Localization of anti eGFP siRNA labeled with Alexa Fluor 546 48h after electrotransfer *in vitro*. Cells in suspension were incubated in the presence of 1.4 μ M siRNA in the pulsing buffer. Ten pulses of 5 ms at frequency of 1 Hz were applied at 0.7 kV/cm. 48 hr after siRNA electrotransfer (+EP) (lower panels), cells were sorted out by flow cytometry and were observed by confocal microscopy with x40 objective. A zoomed picture of one cell is displayed in small boxes. Non-electrotransfected cells (-EP) were observed (top) using the same acquisition parameters. eGFP constitutively expressed in cells was detected with a 488 nm Argon laser (panels on left). Alexa Fluor 546-labeled siRNAs were detected with a 514 nm Helium-Neon laser (central panels). A merged image of the two (panels on right) points to the cytoplasmic localization of the siRNA.

Electrotransfer of siRNAs *in vivo*

When tumors reached an average diameter of 5-7mm a labeled siRNA directed against the eGFP gene (Alexa Fluor 546 eGFP22 siRNA) or an unrelated non-silencing siRNA (negative siRNA) was injected slowly into the mouse tumor. Approximately 30 sec after injection, electric pulses were delivered at 800 V/cm. The higher field intensity was needed due to the skin shunting effect (Mossop et al, 2006). These conditions were chosen as they were previously shown to induce *in vivo* both reporter gene expression (Rols et al, 1998) and siRNA-mediated gene silencing in solid tumors with no tissue damage (Golzio et al, 2007). As reported previously, a muscle contraction was observed when an electric pulse was applied. Neither local burns nor edema or short or long-lived loss of functions were observed in our experiments. When the eGFP22 siRNA was electrotransferred (anti-

GFP+EP), a significant decrease in the eGFP fluorescence of the tumor was observed within 48 hr following the treatment as observed by direct imaging on the animals (Figure 4). The decrease was maximal between days 2 to 4 (data not shown). RNase inhibitor in the injection buffer appeared important, as only a non-statistically significant decrease of the fluorescence was obtained when the inhibitor was absent (data not shown). The decrease of eGFP fluorescence observed upon eGFP22 Alexa labeled siRNA electrotransfer was not observed in the different control groups (Figure 4). Furthermore, electrotransfer of an unrelated siRNA (negative siRNA) did not lead to changes in eGFP expression as compared with the other controls. As expected the electrical treatment itself (PBS+EP) had no effect on eGFP expression in tumor. Interestingly, if no EP were applied after injection of the eGFP22 Alexa labeled siRNA (anti-eGFP-EP) no reduction of the eGFP expression relative to controls was observed. Thus a synergy between the injection and the electrical treatment was needed for efficient delivery of siRNA into tumor cells. Growth of tumors was not affected by any treatment (intratumoral injection of the siRNA and/or EP). This confirmed our previous results showing the same effect (60% of gene expression decrease 48 hr after siRNA electrotransfer) using the same siRNA sequence without the fluorescent-labeling (Golzio et al, 2007). These results further demonstrated that the labeling of the siRNA did not affect its efficacy, *in vivo*.

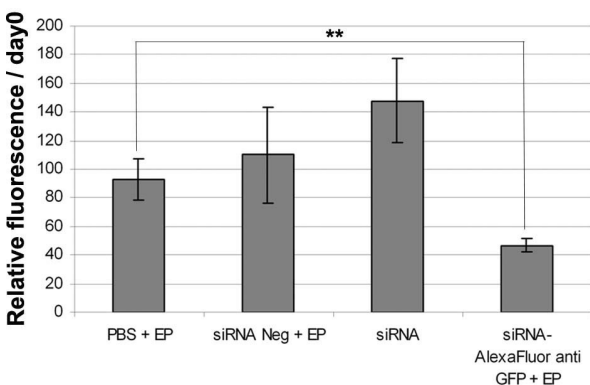


Figure 4. *In vivo* siRNA electrotransfer in B16F10 eGFP tumors. Digital imaging was used to quantify the time lapse fluorescence of B16F10 eGFP tumors. For each animal, the mean fluorescence of the tumor was quantified on a relative scale using as a 100% reference value the fluorescence intensity measured just before treatment (day 0). B16F10 eGFP tumors were injected with either PBS (PBS+EP) or unrelated siRNA (negative siRNA+EP) both injections followed by electrical treatment or injected with the eGFP22 siRNA without or with electrotransfer (anti-eGFP). Differences in fluorescence levels between conditions were statistically compared by using an unpaired t-test two-sided using the Excel software. $^{**}0.05 < P < 0.01$ were plotted when observed. No statistically significant differences ($P > 0.05$) in mean eGFP fluorescence levels were observed between the various samples. Vertical bars represent standard deviation. The number of mice was from three to nine.

Biodistribution of the siRNA after electrotransfer in the tumor

Forty eight hours after the treatment, the mice were euthanized. The tumors were removed and visualized by fluorescence stereomicroscopy. No signal of Alexa Fluor 546 was detected in the non-pulsed tumors (-EP) (Figure 5, upper panels). After electrotransfer of the Alexa labeled siRNA (+EP), GFP fluorescence in the tumors was reduced as compared with the control tumors. Moreover, the Alexa signal was observed to be homogeneously distributed in tumors (Figure 5, lower panels).

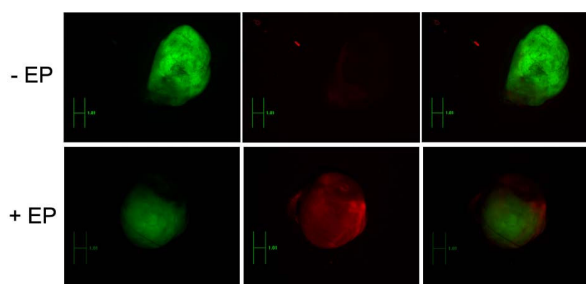


Figure 5. Observation of the anti-eGFP siRNAs labeled with Alexa Fluor 546 after electrotransfer in tumors. 48 hr after electrotransfer (+EP) the tumors were removed and observed under stereo-microscopy, and were compared with the non-electrotransfected tumors (-EP). Left panels, constitutively expressed eGFP; middle panels, siRNA labeled with Alexa Fluor 546; right panels, merged image of left and middle panels (which emphasizes uniform distribution of the siRNA in the tumor).

Localization of the siRNA after electrotransfer in tumors

Histological sections of frozen tumors were observed by confocal microscopy to visualize the expression of eGFP and the localization of labeled siRNAs in the cells (Figure 6). No Alexa fluorescence was detected in non-pulsed tumors (-EP) (Figure 6, upper half). After electrotransfer of the Alexa labeled siRNA (+EP), the eGFP signal of the cells reduced as compared with the control cells. The distribution of the siRNA was homogeneous in electrotransfected tumors, both in the middle as well as on the periphery. At cellular level, the Alexa signal was observed only in the cytoplasm (Figure 6, Lower half). A strong nuclear labeling of a few tumor cells was observed which was consistent with the similar observations *in vitro* in dead cells.

DISCUSSION

RNAi mediated gene-silencing has emerged as a powerful approach for gene function analysis in mammalian cells. Furthermore, the high efficacy of RNAi approaches and fewer side-effects makes them an attractive alternative to antisense oligonucleotides and ribozymes for nucleic acid-based therapies. There are two potential therapeutic RNAi strategies: First approach involves sustained production of

inhibitory RNAs, conferred by replicons, such as plasmids or viral vectors. This approach faces the difficulties encountered by conventional gene therapy methodologies and those associated with the use of viral vectors. The second approach is based on exogenous delivery of chemically synthesized siRNAs, which presents the advantage of terminating the therapeutic treatment in the case of a side-effect, which is not possible for methods involving replicon-based delivery. A lowering in production costs of siRNAs in the past few years further makes them attractive alternatives to small molecule drugs. The main obstacle to the therapeutic application of siRNAs is their *in vivo* delivery. Thus there remains the need of an efficient intracellular delivery method (Dyckhoorn et al, 2006; Rossi, 2005; Xie et al, 2006). Electric pulses induce a major reorganization of the plasma membrane of cells leading to a transient "permeabilized" state (Golzio et al, 2002). This physical technique has been previously used by different groups, including ours, to locally deliver siRNAs in various tissues (Takabatake et al, 2005; Golzio 2005, 2007; Zhang et al, 2002). As previously reported, we observed that the electrical treatment for reversible permeabilization had no detectable effect on tumor growth.

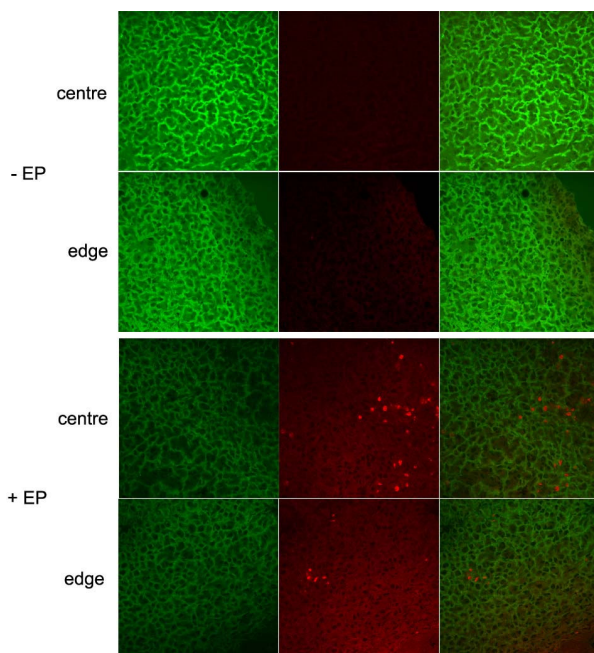


Figure 6. Localization of the anti eGFP siRNAs labeled with Alexa Fluor 546 after electrotransfer in tumors. Forty eight hours after the electrotransfer of the siRNA (+EP) (lower half), the tumors were removed, sliced and observed under a confocal microscope with x40 objective at 0.7 magnification. Non-electrotransfected tumors (-EP) were (top half) compared with electrotransfected tumors. The eGFP expression in cells was detected with a 488 nm Argon laser (left) and the siRNAs labeled with Alexa Fluor 546 were detected with a 514 nm Helium-Neon laser (centre). A merged image of the left and middle panels is shown on in the right panels in order to localize siRNAs.

In this study, we investigated approaches to tracking siRNA upon electrodelivery. Furthermore, we defined experimental systems to visualize and quantify down-regulation of a constitutively expressed eGFP reporter gene, and the localization of siRNAs in subcutaneous B16-F10 melanoma tumors using fluorescence imaging. A similar imaging approach was previously used *in ovo* (Pekarik et al, 2003).

We observed that permeabilization of murine melanoma cells could be achieved by application of long electric pulses, which have been shown to be required for loading macromolecules into cells (Cemazar and Sersa, 2007; Golzio et al, 2007; Rols et al, 1998). As previously observed in many systems, *in vitro* permeabilization of B16F10 cells was only detected for electric field values higher than 300 V/cm (Figure 1). Under such electric pulse conditions, cell viability was only slightly affected by increasing electric field intensity. The optimum electric field intensity (600V/cm) was selected by calculating the percentage of viable permeabilized cells (52%±15).

eGFP signal in cells electrotransfected with siRNAs decreased in the regions of 51% to 57% of the total eGFP expressing cells. This suggests that the level of eGFP expression decreased in most viable cells that had been permeabilized. This observed silencing was neither due to the electric treatment nor the siRNAs alone: Without the application of the electric field, siRNAs failed to enter the cells (Figure 3), and did not show detectable silencing of eGFP expression (Figure 2); furthermore, the electric field alone had no effect on eGFP expression. When the siRNA was electrotransferred, the percentage of eGFP expressing cells decreased significantly at 48 hrs (Figure 2) and the Alexa fluorescence was visualized homogeneously in the cytoplasm of the electro-treated cells (Figure 3). This is in agreement with the cytoplasmic localization of its target (mRNA) (Berezhna et al, 2006; Matsuda and Cepko, 2004). No siRNA was detected in the nucleus of viable cells although it showed considerable affinity for nuclei of dead cells (Figure 6). The silencing of the eGFP expression was significant at 48 hrs as predicted from the life time of the eGFP:24hrs (Corish and Tyler-Smith, 1999). The effectiveness of the anti-eGFP electrotransferred siRNA labeled with Alexa Fluor 546 was transient (data not shown). This could be explained by the short lifetime of this siRNA (that did not carry any stabilizing chemical modification), which could be degraded by intracellular nucleases (Corey, 2007; Elmen et al, 2005; Mook et al, 2007). Moreover, the intracellular concentration of siRNAs is also expected to decrease during cell division (Paroo and Corey, 2004).

Our study of siRNA delivery by electropulsion showed that siRNA molecules had a direct, free access to the cytoplasm (Figures 3 and 6). The other non-viral, chemical delivery methods (such as those involving the use of nanoimmunoliposomes and polyethyleneimine), the uptake mechanism appears to involve the endocytosis pathway, in which siRNA molecules had to escape from the endosomal compartment to access the target mRNAs in the cytoplasm (Pirollo et al, 2007; Jiang et al, 2008). Electrodelivered siRNAs were thus directly available to interact with the

target mRNAs. We anticipate that this direct access may help reduce the induction of off-target effects but this requires further investigation (Crombez et al, 2007).

We also followed the effect of electrical treatment on knockdown of eGFP expression knockdown with siRNAs, *in vivo*. In agreement with a previous report by Filleur et al (2003), we did not observe any detectable reduction in eGFP expression after intratumoral injection of the eGFP22 siRNA alone (Figures 3). eGFP expression knockdown was only observed on the application of electric pulses. The fluorescence imaging data showed that electrical treatment was essential for intracellular uptake of the siRNA following direct intratumoral injection. A key observation was that siRNA appeared distributed homogeneously throughout the cytoplasm of the tumor tissue cells. This suggests that the siRNAs were not being trapped in endosomal compartments. Furthermore, electrotransfer appeared to be affecting all cells in the pulsed volume as a strong inhibition was monitored up to two days after the treatment.

CONCLUSIONS

The direct access to the cytoplasm by siRNAs after electrotransfer emphasizes that this electro-physical method is a powerful tool for effective siRNA delivery, *ex vivo* and *in vivo*.

ACKNOWLEDGMENTS

We thank CNRS CEA Imagerie du petit animal program, the Région Midi-Pyrénées, the Cancéropôle GSO (Grand Sud-Ouest), the InCa (Institut national du Cancer), the ITAV (Institut des techniques avancées du Vivant) and the AFM (Association Française contre les Myopathies) for providing financial resources for this work.

COMPETING INTERESTS

None declared.

REFERENCES

- Aigner A. 2007. Nonviral *in vivo* delivery of therapeutic small interfering RNAs. *Curr Opin Mol Ther*, 9, 345-52.
- Akaneya Y, Jiang B and sumoto TT. 2005. RNAi-induced gene silencing by local electroporation in targeting brain region. *J Neurophysiol*, 93, 594-602.
- Akhtar S and Benter I. 2007. Toxicogenomics of non-viral drug delivery systems for RNAi: potential impact on siRNA-mediated gene silencing activity and specificity. *Adv Drug Deliv Rev*, 59, 164-82.
- Berezna SY, Supekova L, Supek F, Schultz PG and Deniz AA. 2006. siRNA in human cells selectively localizes to target RNA sites. *Proc Natl Acad Sci USA*, 103, 7682-7.
- Caplen NJ, Parrish S, Imani F, Fire A and Morgan RA. 2001. Specific inhibition of gene expression by small double-stranded RNAs in invertebrate and vertebrate systems. *Proc Natl Acad Sci USA*, 98, 9742-7.
- Cemazar M, and Sersa G. 2007. Electrotransfer of therapeutic molecules into tissues. *Curr Opin Mol Ther*, 9, 554-62.
- Cemazar M, Golzio M, Escoffre JM, et al. 2006. *In vivo* imaging of tumor growth after electrochemotherapy with cisplatin. *Biochem Biophys Res Commun*, 348, 997-1002.
- Cemazar M, Sersa G, Wilson J, et al. 2002. Effective gene transfer to solid tumors using different nonviral gene delivery techniques: electroporation, liposomes, and integrin-targeted vector. *Cancer Gene Ther*, 9, 399-406.
- Coralli C, Cemazar M, Kanthou C, Tozer GM and Dachs GU. 2001. Limitations of the reporter green fluorescent protein under simulated tumor conditions. *Cancer Res*, 61, 4784-90.
- Corey DR. 2007. Chemical modification: the key to clinical application of RNA interference? *J Clin Invest*, 117, 3615-22.
- Corish P and Tyler-Smith C. 1999. Attenuation of green fluorescent protein half-life in mammalian cells. *Protein Eng*, 12, 1035-1040.
- Crombez L, Charnet A, Morris MC, Aldrian-Herrada G, Heitz F and Divita G. 2007. A non-covalent peptide-based strategy for siRNA delivery. *Biochem Soc Trans*, 35, 44-6.
- Dyckhoorn DM, Palliser D and Lieberman J. 2006. The silent treatment: siRNAs as small molecule drugs. *Gene Ther*, 13, 541-552.
- Elmen J, Thonberg H, Ljungberg K, Frieden M et al. 2005. Locked nucleic acid (LNA) mediated improvements in siRNA stability and functionality. *Nucleic Acids Res*, 33, 439-47.
- Faurie C, Phez E, Golzio M, Vossen C, Lesbordes JC, Delteil C, Teissie J, and Rols MP. 2004. Effect of electric field vectoriality on electrically mediated gene delivery in mammalian cells. *Biochim Biophys Acta*. 1665, 92-100.
- Filleur S, Courtin A, Ait-Si-Ali S et al. 2003. siRNA-mediated inhibition of vascular endothelial growth factor severely limits tumor resistance to antiangiogenic thrombospondin-1 and slows tumor vascularization and growth. *Cancer Res*, 63, 3919-3922.
- Fire A, Xu S, Montgomery MK, Kostas SA, Driver SE and Mello CC. 1998. Potent and specific genetic interference by double-stranded RNA in *Caenorhabditis elegans*. *Nature*, 391, 806-811.
- Gabriel B and Teissie J. 1995. Spatial compartmentation and time resolution of photooxidation of a cell membrane probe in electropermeabilized Chinese hamster ovary cells. *Eur J Biochem*, 228, 710-8.
- Golzio M, Mazzolini L, Ledoux A et al. 2007. *In vivo* gene silencing in solid tumors by targeted electrically mediated siRNA delivery. *Gene Ther*, 14, 752-9.
- Golzio M, Mazzolini L, Moller P, Rols MP and Teissie J. 2005. Inhibition of gene expression in mice muscle by *in vivo* electrically mediated siRNA delivery. *Gene Ther*, 12, 246-51.
- Golzio M, Teissie J and Rols MP. 2002. Direct visualization at the single-cell level of electrically mediated gene delivery. *Proc Natl Acad Sci USA*, 99, 1292-7.
- Heidel JD, Hu S, Liu XF, Triche TJ and Davis ME. 2004. Lack of interferon response in animals to naked siRNAs. *Nat Biotechnol*, 22, 1579-82.
- Inoue A, Takahashi KA, Mazda O et al. 2005. Electro-transfer of small interfering RNA ameliorated arthritis in rats. *Biochem Biophys Res Commun*, 336, 903-8.
- Jiang G, Park K, Kim J et al. 2008. Hyaluronic acid-polyethyleneimine conjugate for target specific intracellular delivery of siRNA. *Biopolymers*, 89, 635-42.
- Kishida T, Asada H, Gojo S et al. 2004. Sequence-specific gene silencing in murine muscle induced by electroporation-mediated transfer of short interfering RNA. *J Gene Med*, 6, 105-10.
- Li S. 2004. Electroporation gene therapy: new developments *in vivo* and *in vitro*. *Curr Gene Ther*, 4, 309-16.
- Matsuda T and Cepko CL. 2004. Electroporation and RNA interference in the rodent retina *in vivo* and *in vitro*. *Proc Natl Acad Sci USA*, 101, 16-22.
- Miklavcic D, Beravs K, Semrov D, Cemazar M, Demsar F and Sersa G. 1998. The importance of electric field distribution for effective *in vivo* electroporation of tissues. *Biophys J*, 74, 2152-2158.
- Mook OR, Baas F, de Wissel MB and Fluiter K. 2007. Evaluation of locked nucleic acid-modified small interfering RNA *in vitro* and *in vivo*. *Mol Cancer Ther*, 6, 833-43.

- Mossop BJ, Barr RC, Henshaw JW, Zaharoff DA and Yuan F. 2006. Electric fields in tumors exposed to external voltage sources : implication for electric field-mediated drug and gene delivery. *Ann Biomed Eng*, 34, 1564-72.
- Novina CD, and Sharp PA. 2004. The RNAi revolution. *Nature*, 430, 161-4.
- Paroo Z and Corey DR. 2004. Challenges for RNAi in vivo. *Trends Biotechnol*, 22, 390-4.
- Pekarik V, Bourikas D, Miglino N, Joset P, Preiswerk S, Stoeckli ET. 2003 Screening for gene function in chicken embryo using RNAi and electroporation. *Nat Biotechnol*. 21, 93-6.
- Pirollo KF, Rait A, Zhou Q, Hwang SH, Dagata JA, Zon G, Hogrefe RI, Palchik G, Chang EH. 2007 Materializing the potential of small interfering RNA via a tumor-targeting nanodelivery system. *Cancer Res*.67, 2938-43
- Rols MP, Delteil C, Golzio M, Dumond P, Cros S and Teissie J. 1998. In vivo electrically mediated protein and gene transfer in murine melanoma. *Nat Biotechnol* 16, 168-71.
- Rossi J. 2005. Helping RNAi deliver. *Mol Ther*, 11, 653.
- Ryther RC, Flynt AS, Phillips JA and Patton JG. 2005. siRNA therapeutics: big potential from small RNAs. *Gene Ther*, 12, 5-11.
- Takabatake Y, Isaka Y, Mizui M et al. 2005. Exploring RNA interference as a therapeutic strategy for renal disease. *Gene Ther*, 12, 965-73.
- Teissie J, Eynard N, Gabriel B and Rols MP. 1999. Electroporation of cell membranes. *Adv Drug Deliv Rev*, 35, 3-19.
- Wells DJ. 2004. Gene therapy progress and prospects: electroporation and other physical methods. *Gene Ther*, 11, 1363-1369.
- Xie FY, Woodle MC and Lu PY. 2006. Harnessing in vivo siRNA delivery for drug discovery and therapeutic development. *Drug Discov Today*, 11, 67-73.
- Zhang L, Nolan E, Kreitschitz S and Rabussay DP. 2002. Enhanced delivery of naked DNA to the skin by non-invasive in vivo electroporation. *Biochim Biophys Acta*, 1572, 1-9.